

Published in final edited form as:

*Nat Struct Mol Biol.* 2006 January ; 13(1): 63–70.

## Crystal structure and functional analysis of Dcp2p from *Schizosaccharomyces pombe*

Meipei She<sup>1,4</sup>, Carolyn J Decker<sup>2,4</sup>, Nan Chen<sup>1</sup>, Suneeta Tumati<sup>2</sup>, Roy Parker<sup>2</sup>, and Haiwei Song<sup>1,3</sup>

<sup>1</sup> Laboratory of Macromolecular Structure, Institute of Molecular and Cell Biology, 61 Biopolis Drive, Proteos, Singapore 138673

<sup>2</sup> Department of Molecular and Cellular Biology and Howard Hughes Medical Institute, University of Arizona, Tucson, Arizona 85721, USA

<sup>3</sup> Department of Biological Sciences, National University of Singapore, 14 Science Drive, Singapore 117543

### Abstract

Decapping is a key step in both general and nonsense-mediated 5' → ' mRNA-decay pathways. Removal of the cap structure is catalyzed by the Dcp1–Dcp2 complex. The crystal structure of a C-terminally truncated *Schizosaccharomyces pombe* Dcp2p reveals two distinct domains: an all-helical N-terminal domain and a C-terminal domain that is a classic Nudix fold. The C-terminal domain of both *Saccharomyces cerevisiae* and *S. pombe* Dcp2p proteins is sufficient for decapping activity, although the N-terminal domain can affect the efficiency of Dcp2p function. The binding of Dcp2p to Dcp1p is mediated by a conserved surface on its N-terminal domain, and the N-terminal domain is required for Dcp1p to stimulate Dcp2p activity. The flexible nature of the N-terminal domain relative to the C-terminal domain suggests that Dcp1p binding to Dcp2p may regulate Dcp2p activity through conformational changes of the two domains.

mRNA degradation has an important role in post-transcriptional regulation of gene expression. Decapping is a crucial control point in the life of eukaryotic mRNAs, as it permits the degradation of the transcript and is a site of numerous control inputs<sup>1</sup>. For example, transcripts with premature translation termination codons can be degraded by rapid deadenylation-independent decapping<sup>2</sup> in a process referred to as nonsense-mediated decay<sup>3</sup>. In addition, decapping may be important in the AU-rich element (ARE)-mediated decay pathway in mammalian cells, where ARE-binding proteins are thought to recruit the decapping complex and other mRNA-decay enzymes to ARE-containing mRNAs<sup>4,5</sup>. Finally, recent results indicate that the RNA-mediated interference machinery interacts with the decapping enzyme and decapping might have a role in the reduction of mRNA levels by microRNAs<sup>6,7</sup>.

The decapping enzyme complex is composed of Dcp2p (the catalytic subunit) and Dcp1p<sup>8</sup>. Recombinant yeast and human Dcp2 proteins have been shown to have decapping activity<sup>9–11</sup>, with human Dcp2 being a more robust enzyme than its yeast counterpart. Moreover, Dcp2p physically interacts with Dcp1p in human, *S. cerevisiae* and *S. pombe*<sup>9,11–13</sup>, and genetic experiments in yeast indicate that Dcp2p requires Dcp1p to work as a holoenzyme *in vivo*<sup>14,15</sup>. Dcp1p is a small protein containing an EVH1 domain, a protein-protein interaction module

Correspondence should be addressed to R.P. (rpparker@email.arizona.edu) or H.S. (haiwei@imcb.a-star.edu.sg).

<sup>4</sup>These authors contributed equally to this work.

**Accession codes.** Protein Data Bank: Coordinates have been deposited with accession code 2A6T.

**COMPETING INTERESTS STATEMENT**

The authors declare that they have no competing financial interests.

that usually recognizes proline-rich sequences<sup>16</sup>, although the way in which Dcp1p interacts with and affects Dcp2p is not known.

The catalytic subunit, Dcp2p, belongs to the Nudix hydrolase family, all members of which contain the signature Nudix motif<sup>17,18</sup>. Nudix hydrolases are versatile enzymes that catalyze the hydrolysis of nucleoside diphosphates linked to several different moieties and are known to hydrolyze nucleoside triphosphates, nucleotide sugars, dinucleoside polyphosphates, dinucleotide coenzymes and capped mRNAs. The Nudix motif of the Nudix hydrolases functions as a versatile Mg<sup>2+</sup>-binding and catalytic site and forms a loop-helix-loop structure, which is part of a common fold composed of an  $\alpha/\beta/\alpha$ -sandwich called the Nudix fold. The precise catalytic mechanisms of different Nudix hydrolases vary, generally requiring two or three conserved glutamate residues to coordinate a divalent cation crucial for catalysis<sup>18</sup>.

The Nudix motif of Dcp2 has been suggested to be essential for catalysis, as mutation of one of the conserved glutamate residues abolishes decapping activity both *in vivo* and *in vitro*<sup>10–13</sup>. Like many Nudix hydrolases, Dcp2p requires Mg<sup>2+</sup> for activity, although Mn<sup>2+</sup> can increase Dcp2p function *in vitro*<sup>11,19</sup>. Dcp2p is also an RNA-binding protein, and longer RNA is preferred for efficient decapping<sup>9,11,19</sup>. Additional conserved regions termed Box A and Box B, which flank the Nudix motif, have been implicated in phosphate and RNA binding, but their actual functions remain unknown<sup>10,19</sup>.

To gain insight into the molecular basis of decapping, we determined the crystal structure of a C-terminally truncated Dcp2p from *S. pombe*. The structure contains two distinct domains. The C-terminal domain of both *S. cerevisiae* Dcp2p (scDcp2p) and *S. pombe* Dcp2p (spDcp2p) is sufficient for decapping activity. The binding of Dcp2p to Dcp1p is mediated by a conserved hydrophobic surface on its N-terminal domain, and the N-terminal domain is required for Dcp1p to stimulate Dcp2p activity.

## RESULTS

### Structure determination

As the N-terminal ~300 residues of Dcp2 proteins from different organisms are well conserved and essential for decapping<sup>8–10,19</sup>, we expressed and purified a series of C-terminally truncated spDcp2p proteins. All the truncated spDcp2p proteins have decapping activity when assayed *in vitro*. Analytic gel-filtration analysis of the purified Dcp2p proteins indicated that these proteins are monomeric. The truncated proteins were screened for crystallization conditions, and the construct containing the first 266 residues (spDcp2n; residues 1–266) yielded diffraction-quality crystals (Fig. 1a). The crystal structure of spDcp2n was determined by SAD at a resolution of 2.5 Å. The final model contains two molecules (A and B) in the asymmetric unit. Several regions of the polypeptide chain are not visible in the electron density map and are assumed to be disordered, namely residues 79–81, 186–191, 209–214 and 246–266 for molecule A and residues 1–34, 55–57, 69–82, 116–122, 186–191, 209–214 and 244–266 for molecule B.

### Overall structure description

The structure of spDcp2n contains two distinct domains (Fig. 1b), an all- $\alpha$ -helical N-terminal domain and a C-terminal domain containing the Nudix motif. The N-terminal domain (residues 1–93) is formed by six  $\alpha$ -helices and a  $3_{10}$ -helix and is connected by a short hinge linker to the C-terminal domain (residues 98–245). The C-terminal domain consists of a curved central three-stranded mixed  $\beta$ -sheet and a three-stranded antiparallel  $\beta$ -sheet flanked by an  $\alpha$ -helix on both sides, thereby forming an  $\alpha/\beta/\alpha$ -sandwich structure. As in other Nudix hydrolases, the

Nudix sequence motif is located in a loop-helix-loop structure formed by helix  $\alpha 7$  and its connecting loops.

In the crystals of spDcp2n, two molecules are related by two-fold noncrystallographic symmetry in the asymmetric unit. The Nudix domains for the two molecules are very similar, with r.m.s. deviation less than 0.5 Å for all the equivalent C $\alpha$  atoms. In the N-terminal domain of molecule B, only helices  $\alpha 2$ ,  $\alpha 4$  and  $\alpha 6$  are ordered and the rest of the helices are disordered, presumably owing to crystal packing. As no substantial differences were observed between molecules A and B (r.m.s. deviation of 1.2 Å for all the equivalent C $\alpha$  atoms) and molecule A is more complete than molecule B, all subsequent analyses were based on molecule A.

### Structural similarity to other pyrophosphatases

A search of the Protein Data Bank using the Dali server indicated that spDcp2n is highly similar to *Caenorhabditis elegans* Ap4A hydrolase (Ap4AP; PDB entry 1KT9;  $Z = 13.7$ )<sup>20</sup> and *Escherichia coli* ADP-ribose pyrophosphatase (ADPRP; PDB entry 1G0S;  $Z = 13.1$ )<sup>21</sup>, despite the low sequence identities among these proteins. The structural similarity is seen only in the C-terminal Nudix domain of spDcp2n (Fig. 1). Moreover, when a Dali search was carried out using the N-terminal helical domain alone as bait, no structural homolog ( $Z < 4.5$ ) was found, suggesting that the N-terminal domain probably represents a novel fold.

Superposition of the Nudix domain of spDcp2n with those of Ap4AP and ADPRP gives rise to r.m.s. deviation values of 1.6 Å for spDcp2n versus Ap4AP and 1.7 Å for spDcp2n versus ADPRP. The core architectures of the Nudix folds are very similar among these structures (Fig. 1), with the best match being the central  $\beta$ -sheets. The Box B region (residues 217–236) conserved among Dcp2 proteins, which was previously suggested to be outside of the Nudix domain<sup>9,10</sup>, is an essential component of the  $\alpha/\beta/\alpha$ -sandwich structure (Fig. 1b). Box B forms a long  $\alpha$ -helix ( $\alpha 8$ ) that is equivalent to helix  $\alpha 3$  in both Ap4AP and ADPRP (Fig. 1). Consistent with this observation, the minimal fragment of human Dcp2 with RNA-binding and decapping activities contains Box B<sup>19</sup>, presumably because the absence of Box B would destabilize the whole Nudix fold.

Ap4AP is a monomeric protein that hydrolyzes a diphosphate linkage in Ap4A by attacking the P4 phosphate<sup>20</sup>. In Ap4AP, Glu52, Glu56 and Glu103 have been implicated in magnesium binding and nucleophilic attack of the pyrophosphate bond, as a mutation of Glu52, Glu56 or Glu103 to Gln results in a 10<sup>3</sup>-, 10<sup>5</sup>- or 30-fold reduction in  $k_{cat}$  value, respectively<sup>20,22</sup>. Structural comparison shows that residues Glu143 and Glu147 of spDcp2n can be aligned spatially with the Ap4AP active site residues Glu52 and Glu56, respectively, with only small differences in the positions of the side chain groups (Fig. 2a). In contrast, the side chain of Glu192 is pointing away from the catalytic center of spDcp2n, in contrast to its counterpart (Glu103) in the structure of Ap4AP in the binary complex form (Fig. 2a). Glu192 resides near the disordered region (residues 185–191) and is less well defined in the electron density map. Notably, the L6 loop (residues 93–106) containing Glu103 in Ap4AP has no interpretable electron density in the structure of the apo enzyme, and it undergoes a conformational change and becomes ordered upon ligand binding<sup>20</sup>. It is tempting to speculate that the region of residues 185–191 in Dcp2p may become ordered upon substrate binding and the side chain of Glu192 may be oriented to the optimal position for metal binding, catalysis or both. The similarity between the active site structures of spDcp2n and Ap4AP suggests that residues Glu143, Glu147 and Glu192 might have important roles in catalysis.

### The Nudix motif is the catalytic center of Dcp2p

The consensus sequence for the Nudix motif of the Nudix hydrolase family is GX<sub>5</sub>EX<sub>7</sub>REUXEEXGU, in which X is any residue and U is Ile, Leu or Val<sup>17,18</sup>. Although

the precise mechanism of different Nudix hydrolases varies, in general, two or three of the conserved glutamate residues at position 16, 19 and 20 within the Nudix motif are involved in coordinating a divalent cation crucial for catalysis. In addition, one of the glutamates in the motif may act as a general base in catalysis. These sites correspond to Glu143, Glu146 and Glu147 in spDcp2p and Glu149, Glu152 and Glu153 in scDcp2p. Consistent with the Nudix motif being important for Dcp2 catalysis, Glu153 of scDcp2p is required for decapping *in vivo* and *in vitro*<sup>11,12</sup> and its counterpart Glu148 in human Dcp2 is also required for activity *in vitro*<sup>9,10,12</sup>. Similarly, substitution of Glu147 by glutamine abolished the decapping activity of spDcp2p *in vitro* (Fig. 2b). However, it has not been determined whether additional residues within the Nudix motif are required for decapping. Moreover, a glutamate residue (Glu103 in Ap4AP) that is on the C-terminal side of the Nudix box has been found to be important for the activity of several Nudix hydrolases by serving as a general base or by coordinating a divalent cation<sup>18</sup>. Glu192 (Glu198 in *S. cerevisiae*) of spDcp2n could serve such a role, given its structural proximity to other glutamate residues in the Nudix box (Fig. 2a).

To determine whether Glu149 or Glu198 was required for scDcp2p function *in vivo*, we mutated each of these residues to alanine and examined the effect on the decapping of the MFA2pG mRNA, which has a poly(G) tract in its 3' untranslated region (UTR). The poly(G) tract blocks the 5'-to-3' exonuclease, Xrn1p, causing accumulation of a stable intermediate after decapping<sup>23</sup>. The intermediate accumulates in wild-type cells but is reduced or absent in cells deficient in decapping<sup>12,14</sup>. In yeast cells expressing the E149A or E198A mutant alleles of scDcp2p, no decay intermediate was observed, just as in the dcp2Δ strain (Fig. 2c). Therefore, each of these residues is crucial for the activity of scDcp2p. Moreover, mutation of the corresponding residues in spDcp2p, Glu143 or Glu192, to alanine abolished the decapping activity of spDcp2n *in vitro* (Fig. 2b). Together, these results suggest that the Nudix motif is the catalytic center and coordinates with Glu192 (Glu198 in *S. cerevisiae*) for catalysis. Notably, previous results indicate that Glu152 in scDcp2p can be changed to glutamine without affecting function *in vivo*<sup>12</sup>. This suggests that, as in Ap4AP, the glutamate residues in positions 16 and 20 within the Nudix motif in Dcp2p are required for metal coordination.

### Conserved features of the spDcp2n surface

Previous studies have demonstrated that Dcp2p physically interacts with Dcp1p in human, *S. cerevisiae* and *S. pombe*<sup>9,11-13</sup> and that formation of the Dcp1–Dcp2 holoenzyme affects decapping *in vivo* and *in vitro*<sup>11</sup>. To provide insight into the Dcp1p binding site on Dcp2p, we mapped the sequence conservation shared by the Dcp2 proteins across species onto the molecular surface of the spDcp2n structure. This analysis revealed two prominent conserved regions (Fig. 3a). One of the regions is situated in the Nudix domain and corresponds to the Nudix motif, as expected. The other region, formed mainly by residues from Box A (Supplementary Fig. 1 online), is located on one side of the N-terminal helical domain and represents a potential binding site for Dcp1p (Fig. 3a,b).

### The N terminus affects the efficiency of Dcp2p *in vitro*

To determine how the N-terminal domain of spDcp2n functions, we first examined whether it was required for intrinsic decapping activity by testing the decapping activities of the purified spDcp2n lacking either the Nudix domain or the N-terminal domain. The N-terminal domain alone (spDcp2NT; residues 1–95) has no decapping activity, whereas the Nudix domain alone (spDcp2CT; residues 96–266) can decap cap-labeled RNAs, albeit with reduced decapping activity compared to spDcp2n even in the presence of Mn<sup>2+</sup> (Fig. 4). This observation suggests that the N-terminal domain is not absolutely required for the intrinsic decapping activity of spDcp2p protein but can increase spDcp2p function *in vitro*. Moreover, the impaired decapping activity of the Nudix domain cannot be restored by reconstitution of the separately purified N-

and C-terminal domains *in vitro*, as the equimolar mixture of spDcp2NT with spDcp2CT has similar decapping activity to that of spDcp2CT alone (Fig. 4). This result implies that maximal decapping activity of spDcp2p requires the proper orientation and interaction of both domains. Similar results were seen with scDcp2n (residues 1–300), where deletion of the N terminus (residues 1–101; scDcp2ΔN) led to a decrease in decapping activity *in vitro* (Fig. 4).

Additional evidence that the N-terminal domain is not required for catalytic activity but can affect the efficiency of Dcp2p function came from the *in vitro* analysis of point mutations of conserved residues within the N-terminal domains of both the *S. pombe* and *S. cerevisiae* enzymes. These mutations targeted residues within Box A as well as two conserved residues at the C terminus of the N-terminal domain and are all located on the conserved face of the N-terminal domain (Fig. 3a). We observed that although no mutation within the N-terminal domain abolished recombinant Dcp2p function *in vitro*, several residues were required for optimal decapping activity. Specifically, in the spDcp2n enzyme, mutations of Arg18, Phe19, Arg33, Glu39, Trp43, Asp47 and Lys93 to alanine partially decreased the decapping activity in the presence of Mg<sup>2+</sup>, whereas mutation of Phe36 or Phe44 to alanine had little or no substantial effect on the decapping activity (Fig. 5 and Supplementary Table 1 online). Under conditions where Mn<sup>2+</sup> is present, only mutant K93A shows a strong defect in decapping activity (data not shown). The defects of the spDcp2n mutants in decapping are not due to the misfolding of these mutants, as circular dichroism spectroscopy gave very similar spectra for wild-type and mutant spDcp2n proteins (Supplementary Fig. 2 online). Similarly, in scDcp2n, lesions in the corresponding residues generally also had minor effects on decapping activity, with the strongest defects resulting from changes in Arg25 and Arg40, which respectively reduce Dcp2p decapping activity to ~30% and 10% of that of the wild-type enzyme (Fig. 4d,e and Supplementary Table 1).

### The N terminus is indispensable for decapping *in vivo*

To determine whether the N terminus had any important role *in vivo*, we introduced the N-terminal deletion in scDcp2p into a *dcp2Δ* strain and assayed the effect of the deletion on the decapping of the MFA2pG mRNA, as assessed by the abundance of mRNA decay intermediate. As in *dcp2Δ* cells, there was no detectable intermediate present in the cells expressing scDcp2p lacking residues 1–101 (scDcp2ΔN; Fig. 6a). The 1–101 deletion did not reduce the amount of scDcp2p protein (Supplementary Methods and Supplementary Fig. 3 online), therefore the lack of decapping was not due simply to the deletion destabilizing the scDcp2p protein *in vivo*. This result indicates that the N terminus of scDcp2p protein is absolutely required for decapping *in vivo*.

To define what residues in the N-terminal domain are important for decapping *in vivo*, we determined the effects of the point mutations in the N-terminal domain on decapping *in vivo*. Most of the point mutations decreased decapping, but to varying degrees (Fig. 6b, c and Supplementary Table 1). The W50A and D54A mutations had a very strong effect on decapping, causing an approximately eight-fold increase in the ratio of full-length mRNA to the decay fragment. The R25A, Y99A and K100A mutations also caused a strong defect in decapping, increasing the ratio between three- and five-fold, whereas the F26A, R40A, F43A and E46A mutations had only a modest effect on decapping. Finally, mutation of Phe51 to serine did not have any measurable effect on decapping (Supplementary Table 1). Western analysis demonstrated that all these mutant Dcp2p proteins were expressed at levels comparable to that of the wild-type Dcp2p (Supplementary Fig. 3). Thus, scDcp2p function *in vivo* requires specific residues on the conserved surface of the N terminus.

### Dcp1p binds the N-terminal domain of Dcp2p

The strong requirement for the Dcp2 N-terminal domain *in vivo* could be explained if this region was required for the function of Dcp1p, which is the only other protein known to be absolutely required for decapping *in vivo*<sup>14</sup>. To examine possible roles of the N-terminal domain and C-terminal domain in interacting with Dcp1p, we immobilized the spDcp2p deletion variants on glutathione-Sepharose 4B and examined their ability to bind full-length spDcp1p by glutathione *S*-transferase (GST) pull-down assays. The results showed that the N-terminal domain of spDcp2p (spDcp2NT) alone is necessary and sufficient for spDcp1p binding, whereas the Nudix domain (spDcp2CT) is not required for interaction with spDcp1p (Fig. 7a). The association of spDcp2NT with spDcp1p is very tight, as the complex is resistant to high-salt wash (500 mM NaCl). In addition, gel filtration and dynamic light-scattering experiments using purified spDcp2n and spDcp1p confirm this interaction and show they form a complex of 1:1 stoichiometry (data not shown).

To determine what residues within the N-terminal domain were important for binding, we examined whether any of the N-terminal point mutations disrupted the interaction between spDcp1p and spDcp2p. Mutation of Phe19 to alanine abolished spDcp1p binding *in vitro*, and substitution of Arg18 and Phe44 by alanine substantially reduced spDcp1p binding (Fig. 7b and Supplementary Table 1). These results indicate that one function of the conserved patch on the N-terminal domain of spDcp2p is to bind spDcp1p, with residues Arg18, Phe19 and Phe44 being important for this interaction. Similar pull-down experiments were not done with *S. cerevisiae* Dcp1 and Dcp2 proteins because we have been unable to reliably detect a physical interaction between them using recombinant proteins unless they are coexpressed<sup>11</sup>.

To verify these Dcp1p-Dcp2p interactions by a different method, we used a two-hybrid assay to examine what residues of scDcp2p affected scDcp1p interaction. scDcp2n fused to the Gal4 activation domain interacted with scDcp1p fused to the Gal4 DNA-binding domain, as assayed by growth on 3-amino-triazole (3AT)<sup>24</sup> (Fig. 7c). In contrast, scDcp1p does not interact with scDcp2p lacking the entire N-terminal domain (scDcp2ΔN). When the activation-domain fusions with scDcp2p containing point mutations in the N terminus were tested, mutations in Arg25, Phe26 and Phe51 disrupted the interaction between Dcp2p and Dcp1p, as judged by lack of growth on 3AT. The other point mutations tested had no detectable effect on the two-hybrid interaction between Dcp2p and Dcp1p. Notably, Arg25, Phe26 and Phe51 in scDcp2p correspond to Arg18, Phe19 and Phe44 in spDcp2p, which affected Dcp1p-Dcp2p interaction *in vitro*. Therefore, multiple assays identify the same conserved residues as being important for Dcp1p-Dcp2p interaction.

### Dcp1p stimulates Dcp2p decapping activity *in vitro*

To determine the functional significance of the interaction of Dcp1p with the N-terminal domain of Dcp2p, we first demonstrated that recombinant Dcp1p could stimulate Dcp2p activity *in vitro* for both spDcp2n and scDcp2n. For example, spDcp2n has robust decapping activity in the presence of Mn<sup>2+</sup> and has weaker decapping activity in the presence of Mg<sup>2+</sup>, which is stimulated by the addition of spDcp1p (Fig. 5a–d). Moreover, the spDcp2p mutants R18A, F19A and F44A, which have strong defects in spDcp1p binding (Fig. 7b), were not stimulated by spDcp1p (Fig. 5a, b and Supplementary Table 1), indicating that the stimulation of Dcp2p by Dcp1p requires interaction of the proteins. The inability of R18A, F19A and F44A to be stimulated by spDcp1p was not due to the reduced decapping activities of these mutants, as mutants R33A, E39A and W43A all have reduced activity yet are still stimulated by spDcp1p and capable of binding spDcp1p (Figs. 5 and 7).

Similar, but not identical, results were seen with scDcp2n. scDcp2n has very weak activity in the presence of Mg<sup>2+</sup>, which is increased substantially by the addition of scDcp1p (Fig. 5e, f).

For scDcp2n, a wider spectrum of mutations in the N-terminal domain affected the ability of Dcp1p to stimulate the enzyme. Specifically, scDcp1p did not stimulate the R25A, F26A, E46A, W50A, F51S, D54A or K100A mutants of scDcp2n (Fig. 5e, f and Supplementary Table 1). Mutants R25A, F26A and F51S, corresponding to mutants R18A, F19A and F44A in spDcp2p, respectively, have strong defects in scDcp1p binding (Fig. 7c). The wider spectrum of alleles affecting Dcp1p activity in the *S. cerevisiae* enzymes compared to those of *S. pombe* may result from the weaker activity of scDcp2n by itself when compared to spDcp2n; spDcp2n is markedly more active than scDcp2n in the presence of Mg<sup>2+</sup>. In contrast to the other mutants, the scDcp2n proteins with the R40A and F43A mutations were stimulated by the addition of scDcp1p (Fig. 5e, f), which is consistent with these positions not affecting binding between Dcp1p and Dcp2p in both *S. cerevisiae* and *S. pombe* (Fig. 7b, c and Supplementary Table 1). Together, the results with both the spDcp2n and scDcp2n enzymes indicate that Dcp1p stimulates the decapping activity of Dcp2p through its physical interaction with the N-terminal domain of Dcp2p.

## DISCUSSION

The mechanism by which Dcp1p stimulates the decapping activity of Dcp2p remains elusive. One possibility is that Dcp1p interacts with the N-terminal domain of Dcp2p to induce a conformational change within or between the two Dcp2p domains, thereby increasing Dcp2p's substrate recognition, catalytic activity or both. Given that the two domains of Dcp2p are connected by a flexible loop, the binding of Dcp1p might lead to a reorientation of these two domains, thereby increasing the interaction of substrate with Dcp2p. Two lines of evidence suggest that Dcp1p may contribute to decapping directly, perhaps by interactions with the substrate. First, Asp31 and Arg70 in scDcp1p are crucial for the decapping activity of the Dcp1p–Dcp2p complex but are not involved in complex formation<sup>16</sup>. Second, two temperature-sensitive mutants of spDcp1p block mRNA decapping *in vivo* but still co-immunopurify with Dcp2p<sup>15</sup>. Our hypothesis is that Dcp1p stimulates decapping both by interactions with the substrate and by affecting the conformation of Dcp2p.

Our results suggest that the N-terminal domain of Dcp2p also functions independently of Dcp1p to increase the decapping efficiency. As the specificities of other Nudix hydrolases are conferred by insertions into and/or extensions of the basic Nudix fold<sup>18</sup>, one possible role of the N-terminal domain might be to provide additional contacts for substrate binding. Consistent with the N-terminal domain affecting substrate binding, removal of the N-terminal domain from human Dcp2 leads to decreased substrate specificity<sup>19</sup>.

One notable feature of Dcp2p is that there is not always a strict correlation between mutations that affect Dcp1p–Dcp2p binding and/or function in *in vitro* and *in vivo* assays of overall decapping efficiency. For example, the R40A, F43A, W50A, D54A, Y99A and K100A mutations in scDcp2p still allow Dcp1p–Dcp2p interaction, either in *in vitro* biochemical assays with the corresponding mutations in spDcp2p or in *in vivo* two-hybrid assays; yet they result in defects in decapping *in vivo*. This result provides additional evidence that the N-terminal domain has functions in promoting decapping in addition to binding Dcp1p, possibly in the form of additional interactions required for Dcp1p to stimulate Dcp2p activity after binding. By contrast, we found that the R25A, F26A and F51S mutations, which weakened Dcp1p–Dcp2p interactions for both spDcp1–spDcp2p *in vitro* and scDcp1–scDcp2 in the two-hybrid assay, decreased decapping *in vivo* only moderately (R25A), mildly (F26A) or not detectably (F51S). A likely explanation for this discrepancy is that point mutations weakening the interaction between Dcp1p and Dcp2p are stabilized *in vivo* by interactions with additional components of the larger decapping complex.

Dcp2p has been reported to be an RNA-binding protein<sup>19</sup>. However, no positively charged patch large enough for potential RNA binding was observed on the molecular surface of spDcp2n. Therefore, the RNA-binding site on Dcp2p remains to be determined. Further crystallographic, biochemical and genetic studies of the Dcp1p–Dcp2p complex are required to elucidate the catalytic mechanism of mRNA decapping.

## METHODS

### Construction of Dcp2 plasmids and mutagenesis

The DNA segments encoding spDcp2n (residues 1–266), spDcp2CT (96–266), spDcp2NT (1–95) and spDcp1p were PCR amplified from *S. pombe* genomic DNA and cloned into pGEX-6p-1. The DNA encoding scDcp2p (1–970) in *S. cerevisiae* was PCR amplified from pRP925 (ref. 12) and cloned into pRP10 (ref. 25) to produce pRP1207. The plasmid pRP1210 expressing scDcp2n (1–300), which is His-tagged at the N terminus and Flag-tagged at the C terminus, was constructed by PCR amplification using oRP1126 (ref. 11) and oRP1253 followed by insertion of the product into pPROEX-1 (Gibco BRL). Plasmids to express point mutants of scDcp2n were constructed in the same way using the mutant pRP1207 derivatives as templates. The plasmid to express scDcp2p $\Delta$ N (102–300), pRP1211, was constructed by PCR amplification using oRP1252, oRP1253 and pRP1210 followed by insertion of the product into pPROEX-1. Point mutations in spDcp2p and scDcp2p were created using the QuikChange mutagenesis method (Stratagene). All mutated constructs were verified by DNA sequencing.

### Protein purification

GST-tagged spDcp2n was expressed in *E. coli* and purified using glutathione-Sepharose 4B, MonoS and Superdex-75 columns (Amersham). Selenomethionine (SeMet)-substituted spDcp2n was purified in the same way except that 20 mM DTT was used. Mutants of spDcp2n were purified by glutathione-Sepharose 4B and the GST tag was then removed. spDcp1p was purified using glutathione-Sepharose 4B, MonoQ and Superdex-75 columns. scDcp2n was expressed from pRP1210 in *E. coli* BL21 and purified from inclusion bodies under denaturing conditions using 4M urea and His-bind resin (Novagen). Purified protein was then renatured, dialyzed and stored as described before<sup>19</sup> except the storage buffer did not contain magnesium acetate or DTT. Mutants of scDcp2n were purified in the same manner. His-tagged full-length scDcp1p was expressed from pRP785 (ref. 11) in *E. coli* DH5 $\alpha$ , purified using His-bind resin under native conditions and stored in 20 mM Tris-HCl (pH 7.5), 100 mM NaCl, 10% (v/v) glycerol and 1mM DTT.

### Crystallization, data collection and structure determination

spDcp2n crystals were grown at 20°C by hanging drop vapor diffusion. An equal volume of protein was mixed with the precipitant solution (5% (w/v) PEG 200, 1.4 M NaH<sub>2</sub>PO<sub>4</sub>, 0.6 M K<sub>2</sub>HPO<sub>4</sub>). SeMet-substituted crystals were grown under the same conditions. Before data collection, crystals were transferred stepwise to a cryo-buffer (2.5 M malonic acid (pH 6.5), 5% (w/v) PEG 200) and flash-frozen in liquid nitrogen. Crystals belonged to space group *P*6<sub>1</sub> with two molecules per asymmetric unit.

Native and SeMet SAD data ( $\lambda = 0.9798 \text{ \AA}$ ) were collected at beamline ID29 (European Synchrotron Radiation Facility). Data were processed with CCP4 programs<sup>26</sup>. SOLVE<sup>27</sup> and SHARP<sup>28</sup> were used to locate 14 of 16 selenium sites in the asymmetric unit. After solvent flattening, a partial model built with RESOLVE<sup>29</sup> was used for manual model building with O<sup>30</sup>. The model was refined with CNS<sup>31</sup> and then REFMAC5 (ref. 31) using the native data set at a resolution of 2.5 Å. The final model has a good stereochemistry with a free *R*-factor of

28.7% and an *R*-factor of 25.0%. The data collection and refinement statistics are shown in Table 1.

### GST pull-down assay

The full length spDcp1p was expressed as a GST-fusion protein in the *E. coli* BL21 strain. Clarified cell lysate was incubated with glutathione-Sepharose 4B beads at 4°C for 1 h. After centrifugation, the beads were washed three times with the binding buffer (20 mM Tris-HCl (pH 7.6), 150 mM NaCl, 2 mM DTT). The beads were then aliquoted and incubated with purified wild-type and mutant spDcp2n proteins for 1 h on ice. Supernatants were removed and beads were washed extensively with the binding buffer. Proteins eluted from beads with 20 mM glutathione in the binding buffer were resolved by 15% (v/v) SDS-PAGE and visualized by Coomassie blue staining.

### Two-hybrid analysis

scDcp2n, scDcp2ΔN and derivatives of scDcp2n carrying point mutations in the N terminus were inserted into pOAD and scDcp1 was inserted into pOBD2 (ref. 24). Yeast strains PJ69-4A and PJ69-4α<sup>32</sup> containing the pOAD-Dcp2 and the pOBD2-Dcp1 plasmids, respectively, were mated. Growth of the diploids was assayed on minimal selective media lacking leucine, tryptophan and histidine and containing 100 mM 3AT.

### Decapping assays

For decapping assays with spDcp2n, uncapped RNA was transcribed using the Ampliscribe T7 transcription kit (Epicentre Technologies) with the control linear λ DNA in the kit as a template. [ $\alpha$ -<sup>32</sup>P]GTP-labeled capping of the 1.5-kilobase RNA fragment was carried out as described in ref. <sup>33</sup>. All experiments were carried out in a buffer containing 50 mM Tris-HCl (pH 7.9), 30 mM ammonium sulfate and 1 mM MgCl<sub>2</sub>. For experiments with Mn<sup>2+</sup>, 0.5 mM MnCl<sub>2</sub> was included in addition to 1 mM MgCl<sub>2</sub>. Generally, 3 pmol of wild-type or mutant spDcp2n was used in each 18-μl reaction. For experiments with spDcp1p, proteins were mixed in the reaction buffer and incubated on ice for 30 min before capped RNA was added. The decapping reaction was carried out at 37°C for 30 min, then stopped by 25 mM EDTA.

For decapping assays with scDcp2n, uncapped RNA was transcribed and purified from MnlI-digested pRP802 as described in ref. <sup>34</sup>. The 99-nucleotide RNA was capped using guanylyltransferase (Ambion) and [ $\alpha$ -<sup>32</sup>P]GTP according to the manufacturer's instructions. Decapping was assayed in 20-μl reactions containing 20 fmol cap-labeled RNA, 50 mM HEPES (pH 7.0), 100 mM NaCl and 2 mM DTT. Intrinsic decapping activity was assayed in 2 mM MnCl<sub>2</sub> with 20 ng scDcp2n and 80 ng BSA (Roche). Stimulation by scDcp1p was assayed in 5 mM MgCl<sub>2</sub> with 100 ng scDcp2n and either 300 ng scDcp1p or 300 ng BSA. Reaction mixes were preheated at 30°C for 2 min before the addition of proteins, incubated for 10 min at 30°C then stopped by the addition of 10 μl 0.5 M EDTA. Dcp1p or BSA was added just before Dcp2p. Aliquots of the reaction products from both types of decapping assays were spotted on polyethyleneimine-cellulose TLC plates (Sigma or Baker) and developed in 0.75 M LiCl.

### In vivo mRNA analysis

*S. cerevisiae* strain yRP2061 (*Mataura3-52 lys2-201 leu2-3 trp1 cup1::LEU2(PM) dcp2::TRP1*) carrying plasmids expressing wild-type or mutant versions of scDcp2p was grown to an OD<sub>600</sub> of 0.3–0.4 in synthetic media lacking uracil and containing 2% (w/v) galactose. Total RNA was isolated as described in ref. <sup>35</sup> and was fractionated on 1.75% (w/v) formaldehyde agarose gels. MFA2pG mRNA and its decay fragment were detected by northern analysis using oRP140 (ref. 36).

## Supplementary Material

Refer to Web version on PubMed Central for supplementary material.

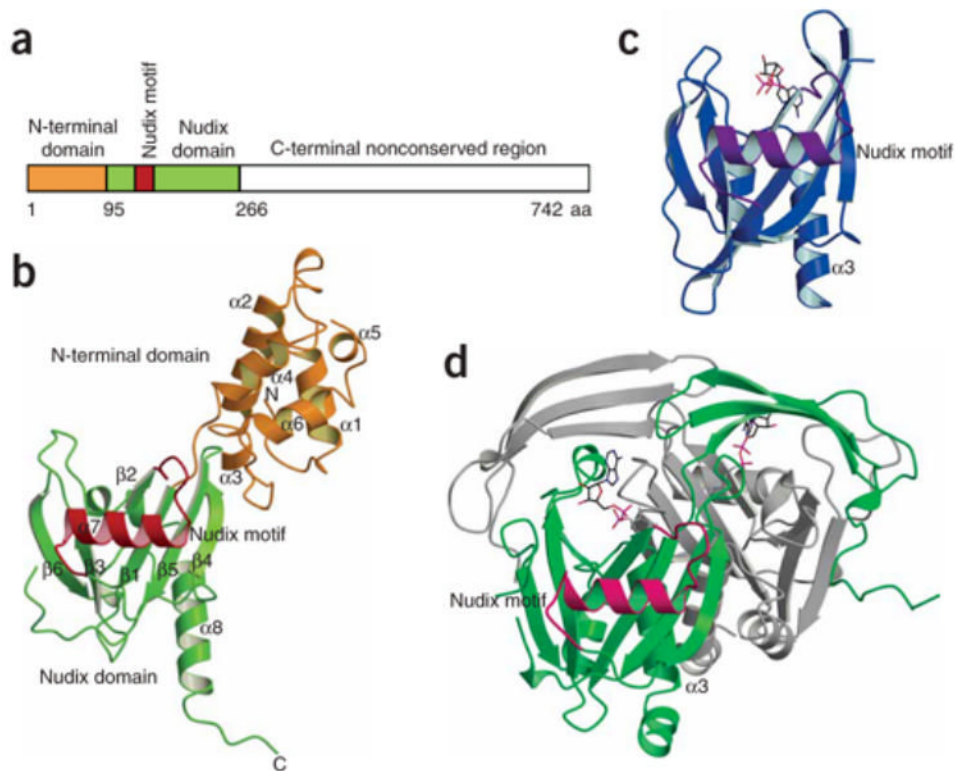
### Acknowledgements

We would like to thank the beamline scientists at ID29 (European Synchrotron Radiation Facility) for assistance and access to their facilities. Plasmids and yeast strains used for the two-hybrid analysis were provided by S. Fields, Howard Hughes Medical Institute, University of Washington. pRP2075 was provided by J. Collier, Howard Hughes Medical Institute, University of Arizona. This work was financially supported by the Agency for Science, Technology and Research (A\* Star) in Singapore (H.S.) and by the Howard Hughes Medical Institute (R.P.).

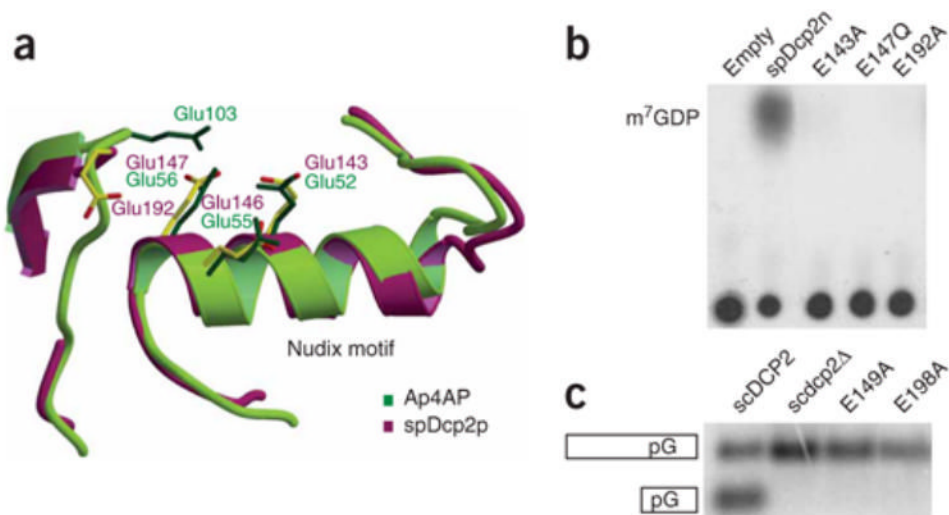
### References

1. Parker R, Song H. The enzymes and control of eukaryotic mRNA turnover. *Nat Struct Mol Biol* 2004;11:121–127. [PubMed: 14749774]
2. Muhlrad D, Parker R. Premature translational termination triggers mRNA decapping. *Nature* 1994;370:578–581. [PubMed: 8052314]
3. Maquat LE. Nonsense-mediated mRNA decay: splicing, translation and mRNP dynamics. *Nat Rev Mol Cell Biol* 2004;5:89–99. [PubMed: 15040442]
4. Lykke-Andersen J, Wagner E. Recruitment and activation of mRNA decay enzymes by two ARE-mediated decay activation domains in the proteins TTP and BRF-1. *Genes Dev* 2005;19:351–361. [PubMed: 15687258]
5. Gao M, Wilusz CJ, Peltz SW, Wilusz J. A novel mRNA-decapping activity in HeLa cytoplasmic extracts is regulated by AU-rich elements. *EMBO J* 2001;20:1134–1143. [PubMed: 11230136]
6. Sen GL, Blau HM. Argonaute 2/RISC resides in sites of mammalian mRNA decay known as cytoplasmic bodies. *Nat Cell Biol* 2005;7:633–636. [PubMed: 15908945]
7. Liu J, Valencia-Sanchez MA, Hannon GJ, Parker R. MicroRNA-dependent localization of targeted mRNAs to mammalian P-bodies. *Nat Cell Biol* 2005;7:719–723. [PubMed: 15937477]
8. Collier J, Parker R. Eukaryotic mRNA decapping. *Annu Rev Biochem* 2004;73:861–890. [PubMed: 15189161]
9. van Dijk E, et al. Human Dcp2: a catalytically active mRNA decapping enzyme located in specific cytoplasmic structures. *EMBO J* 2002;21:6915–6924. [PubMed: 12486012]
10. Wang Z, Jiao X, Carr-Schmid A, Kiledjian M. The hDcp2 protein is a mammalian mRNA decapping enzyme. *Proc Natl Acad Sci USA* 2002;99:12663–12668. [PubMed: 12218187]
11. Steiger M, Carr-Schmid A, Schwartz DC, Kiledjian M, Parker R. Analysis of recombinant yeast decapping enzyme. *RNA* 2003;9:231–238. [PubMed: 12554866]
12. Dunckley T, Parker R. The DCP2 protein is required for mRNA decapping in *Saccharomyces cerevisiae* and contains a functional MutT motif. *EMBO J* 1999;18:5411–5422. [PubMed: 10508173]
13. Lykke-Andersen J. Identification of a human decapping complex associated with hUpf proteins in nonsense-mediated decay. *Mol Cell Biol* 2002;22:8114–8121. [PubMed: 12417715]
14. Beelman CA, et al. An essential component of the decapping enzyme required for normal rates of mRNA turnover. *Nature* 1996;382:642–646. [PubMed: 8757137]
15. Sakuno T, et al. Decapping reaction of mRNA requires Dcp1 in fission yeast: its characterization in different species from yeast to human. *J Biochem* 2004;136:805–812. [PubMed: 15671491]
16. She M, et al. Crystal structure of Dcp1p and its functional implications in mRNA decapping. *Nat Struct Mol Biol* 2004;11:249–256. [PubMed: 14758354]
17. Bessman MJ, Frick DN, O’Handley SF. The MutT proteins or “Nudix” hydrolases, a family of versatile, widely distributed, “housecleaning” enzymes. *J Biol Chem* 1996;271:25059–25062. [PubMed: 8810257]
18. Mildvan AS, et al. Structures and mechanisms of Nudix hydrolases. *Arch Biochem Biophys* 2005;433:129–143. [PubMed: 15581572]
19. Piccirillo C, Khanna R, Kiledjian M. Functional characterization of the mammalian mRNA decapping enzyme hDcp2. *RNA* 2003;9:1138–1147. [PubMed: 12923261]

20. Bailey S, et al. The crystal structure of diadenosine tetraphosphate hydrolase from *Caenorhabditis elegans* in free and binary complex forms. *Structure (Camb)* 2002;10:589–600. [PubMed: 11937063]
21. Gabelli SB, Bianchet MA, Bessman MJ, Amzel LM. The structure of ADP-ribose pyrophosphatase reveals the structural basis for the versatility of the Nudix family. *Nat Struct Biol* 2001;8:467–472. [PubMed: 11323725]
22. Abdelghany HM, Bailey S, Blackburn GM, Rafferty JB, McLennan AG. Analysis of the catalytic and binding residues of the diadenosine tetraphosphate pyrophosphohydrolase from *Caenorhabditis elegans* by site-directed mutagenesis. *J Biol Chem* 2003;278:4435–4439. [PubMed: 12475970]
23. Decker CJ, Parker R. A turnover pathway for both stable and unstable mRNAs in yeast: evidence for a requirement for deadenylation. *Genes Dev* 1993;7:1632–1643. [PubMed: 8393418]
24. Cagney G, Uetz P, Fields S. High-throughput screening for protein-protein interactions using two-hybrid assay. *Methods Enzymol* 2000;328:3–14. [PubMed: 11075334]
25. Heaton B, et al. Analysis of chimeric mRNAs derived from the STE3 mRNA identifies multiple regions within yeast mRNAs that modulate mRNA decay. *Nucleic Acids Res* 1992;20:5365–5373. [PubMed: 1437553]
26. Collaborative Computational Project, Number 4. The CCP4 suite: programs for protein crystallography. *Acta Crystallogr D Biol Crystallogr* 1994;50:760–763. [PubMed: 15299374]
27. Terwilliger TC, Berendzen J. Automated MAD and MIR structure solution. *Acta Crystallogr D Biol Crystallogr* 1999;55:849–861. [PubMed: 10089316]
28. De la Fortelle E, Bricogne G. Maximum-likelihood heavy-atom parameter refinement for multiple isomorphous replacement and multiwavelength anomalous diffraction method. *Methods Enzymol* 1997;276:472–494.
29. Terwilliger TC. Automated structure solution, density modification and model building. *Acta Crystallogr D Biol Crystallogr* 2002;58:1937–1940. [PubMed: 12393925]
30. Jones TA, Zou JY, Cowan SW, Kjeldgaard M. Improved methods for building protein models in electron density maps and the location of errors in these models. *Acta Crystallogr A* 1991;47:110–119. [PubMed: 2025413]
31. Brunger AT, et al. Crystallography & NMR system: A new software suite for macro-molecular structure determination. *Acta Crystallogr D Biol Crystallogr* 1998;54:905–921. [PubMed: 9757107]
32. James P, Halladay J, Craig EA. Genomic libraries and a host strain designed for highly efficient two-hybrid selection in yeast. *Genetics* 1996;144:1425–1436. [PubMed: 8978031]
33. Zhang S, Williams CJ, Wormington M, Stevens A, Peltz SW. Monitoring mRNA decapping activity. *Methods* 1999;17:46–51. [PubMed: 10075882]
34. LaGrandeur TE, Parker R. Isolation and characterization of Dcp1p, the yeast mRNA decapping enzyme. *EMBO J* 1998;17:1487–1496. [PubMed: 9482745]
35. Caponigro G, Muhlrud D, Parker R. A small segment of the MAT alpha 1 transcript promotes mRNA decay in *Saccharomyces cerevisiae*: a stimulatory role for rare codons. *Mol Cell Biol* 1993;13:5141–5148. [PubMed: 8355674]
36. Caponigro G, Parker R. Multiple functions for the poly(A)-binding protein in mRNA decapping and deadenylation in yeast. *Genes Dev* 1995;9:2421–2432. [PubMed: 7557393]

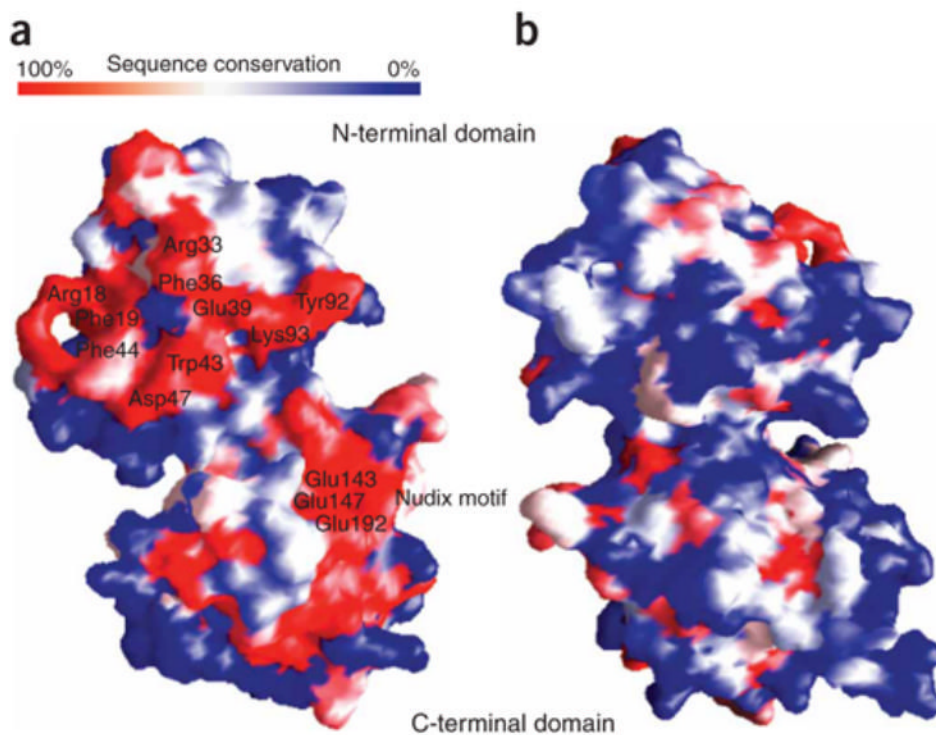


**Figure 1.** Crystal structure of spDcp2n and comparison with other Nudix enzymes. **(a)** Schematic representation of the domain organization of Dcp2p from *S. pombe*. **(b)** Ribbon diagram of spDcp2n. Orange, the N-terminal helical domain; light green, the C-terminal Nudix domain; red, the Nudix motif. Secondary structure elements are labeled. **(c)** Structure of Ap4AP in complex with a phosphate and AMP (PDB entry 1KTG). Sticks, AMP and phosphates; purple, the Nudix motif. **(d)** Structure of ADPRP in complex with ADP-ribose (PDB entry 1G9Q). Green, subunit A; gray, subunit B; sticks, ADP-ribose; magenta, the Nudix motif. The view of the Nudix domain for subunit A is the same as those for spDcp2n and Ap4AP.

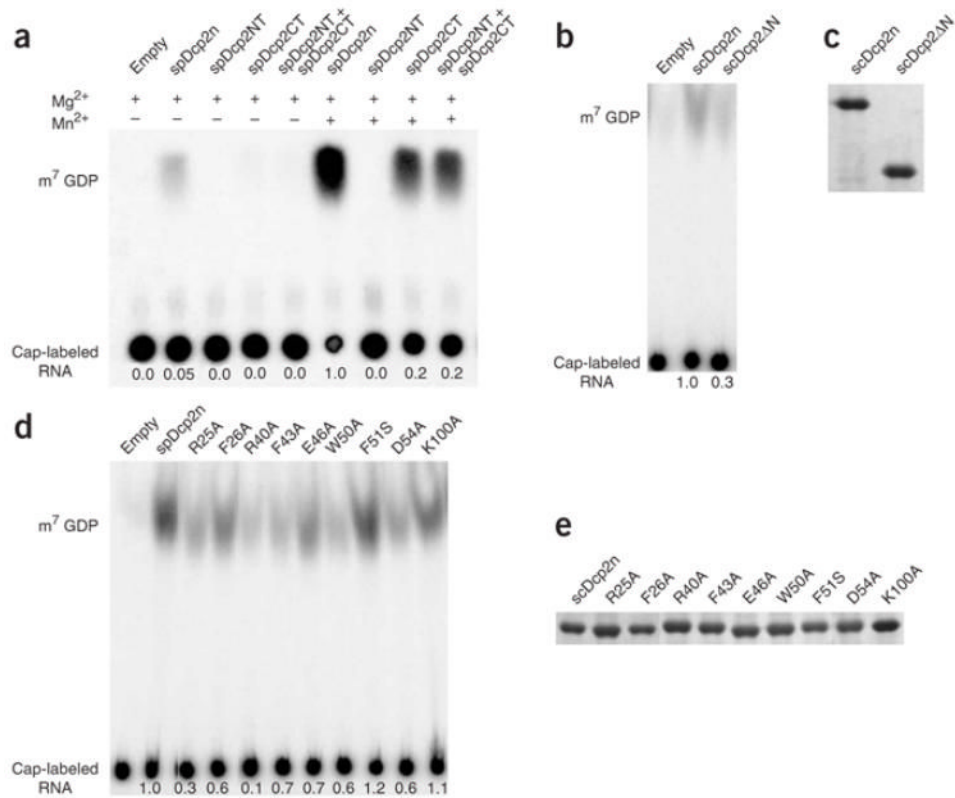


**Figure 2.**

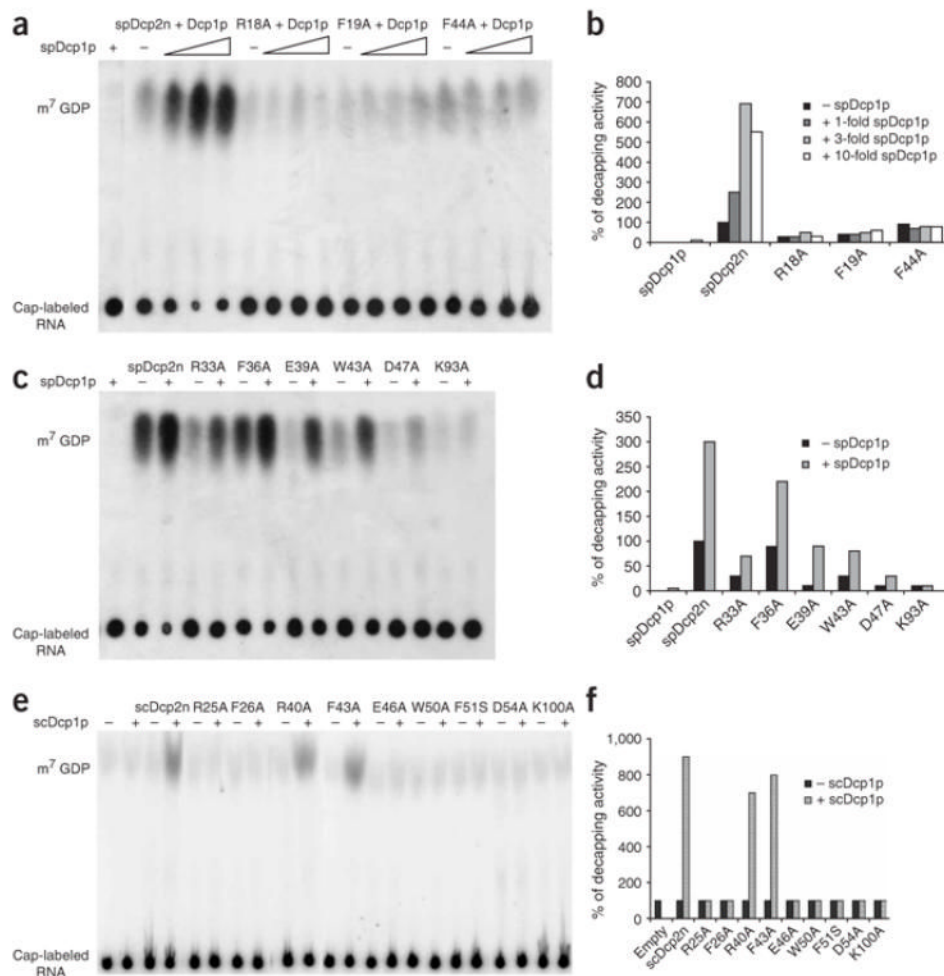
The Nudix motif of spDcp2n is a catalytic center. **(a)** Superposition of the Nudix motifs of spDcp2n (purple) and Ap4AP (green). Residues involved in catalysis are shown as stick models. **(b)** *In vitro* decapping assays of wild-type spDcp2n and mutant spDcp2n proteins in which conserved glutamate residues in the Nudix motif were substituted by alanine. **(c)** Northern analysis of steady-state levels of full-length MFA2 mRNA with poly(G) inserted in the 3' UTR and of the decay intermediate in cells expressing *S. cerevisiae* wild-type Dcp2p (scDCP2), no Dcp2p (scdcp2 $\Delta$ ) or Dcp2 proteins with single-amino acid substitutions for glutamate residues in the Nudix motif.



**Figure 3.** Surface views of spDcp2n. **(a)** Surface representation of spDcp2n showing the regions of high to low sequence conservation among the eukaryotic Dcp2 proteins. Besides the highly conserved Nudix motif, a large conserved patch in the N-terminal domain is revealed and corresponding residues are labeled. **(b)** Back view of the molecular surface of spDcp2n showing the sequence conservation. The molecule is rotated 180° along a vertical axis relative to the view in **a**.

**Figure 4.**

The N-terminal domain affects the efficiency of Dcp2p *in vitro*. **(a)** Decapping assays of wild-type spDcp2n and deletion mutants of spDcp2n in the presence of Mg<sup>2+</sup>, Mn<sup>2+</sup> or both. Numbers below lanes in **a**, **b** and **d** indicate decapping activity relative to wild-type proteins (average of at least two independent measurements). **(b)** Decapping assay in the presence of Mn<sup>2+</sup> using purified wild-type scDcp2p residues 1–300 (scDcp2n) or residues 102–300 (scDcp2ΔN). **(c)** Silver-stain analysis of aliquots of purified scDcp2n and scDcp2ΔN proteins used in the decapping assays in **b**. **(d)** Decapping assay in the presence of Mn<sup>2+</sup> using purified wild-type scDcp2n or scDcp2n proteins containing single-residue substitutions in the N terminus. **(e)** Silver-stain analysis of aliquots of the purified wild-type and mutant scDcp2n proteins used in the decapping assays in **d**.

**Figure 5.**

The N-terminal domain of Dcp2p is required for Dcp1p to stimulate decapping. **(a)** Effects of spDcp1p on the decapping activities of wild-type and mutant spDcp2n proteins in the presence of Mg<sup>2+</sup>. Wild-type or mutant spDcp2n protein (3 pmol) plus spDcp1p at a 1-, 3- or 10-fold molar ratio relative to spDcp2n or its mutants were used in the decapping assay; triangles denote increase in spDcp1p concentration. **(b)** Quantification of the stimulation effects shown in **a**. **(c)** Decapping assay of mutant spDcp2n proteins with single mutations in the conserved patch of the N-terminal domain in the absence or presence of spDcp1p. 3 pmol of both wild-type and mutant spDcp2n proteins and 18 pmol spDcp1p were used. **(d)** Quantification of the decapping activities shown in **c**. **(e)** Decapping assay in the presence of Mg<sup>2+</sup> using purified wild-type scDcp2n or scDcp2n proteins containing single-amino acid substitutions in the N terminus in the presence of scDcp1p (+) or BSA (-). **(f)** Quantification of the decapping activities shown in **e**.

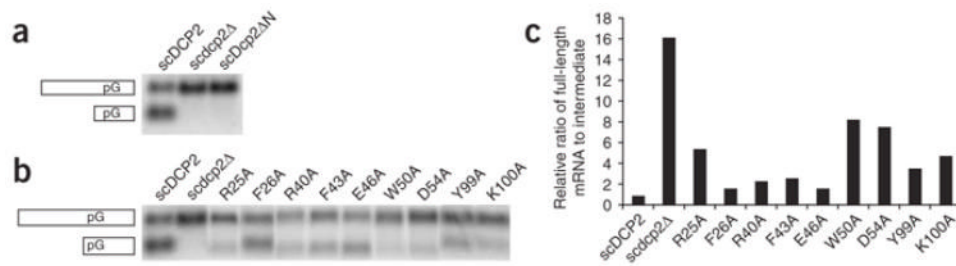


**Figure 6.**

The N terminus of Dcp2p is absolutely required *in vivo* for decapping. (a) Northern analysis of steady-state level of full-length MFA2 mRNA containing poly(G) in its 3' UTR and that of its decay intermediate produced by decapping and 5'-to-3' exonucleolytic digestion, in cells expressing wild-type *S. cerevisiae* Dcp2p (scDCP2), no Dcp2p (scdcp2Δ) or Dcp2p lacking the N-terminal 101 residues (scDcp2ΔN). (b) Northern analysis of steady-state levels of full-length MFA2 mRNA and decay intermediate in cells expressing scDCP2, scdcp2Δ or scDcp2p proteins with single-amino acid substitutions in the N terminus. (c) Histogram showing the ratio of full-length mRNA to intermediate relative to the ratio seen in wild-type cells (set to 1).

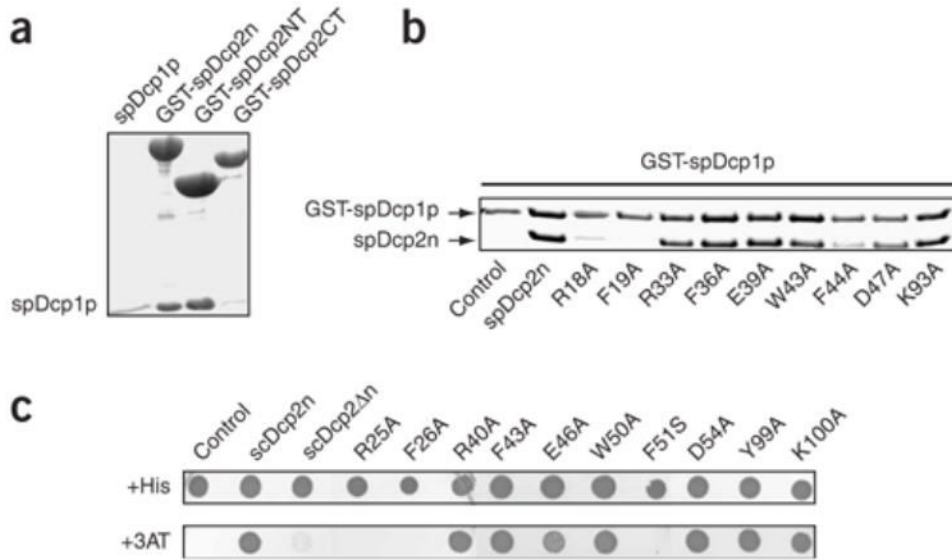


**Figure 7.** Dcp1p interacts with the N-terminal domain of Dcp2p. **(a)** GST pull-down results showing that both GST-spDcp2n and GST-Dcp2NT bind recombinant spDcp1p, whereas the binding of spDcp1p to GST-Dcp2CT is greatly reduced. **(b)** GST pull-down results showing binding of GST-tagged spDcp1p to tag-free wild-type (WT) and mutant spDcp2n proteins with single residues substituted to alanine in the N-terminal conserved patch. Control lane contains purified GST-spDcp1p alone. In **a** and **b**, proteins were resolved by SDS-PAGE and visualized by Coomassie blue staining. **(c)** Two-hybrid analysis of the interaction between scDcp1 fused to the Gal4 DNA-binding domain and scDcp2n fused to the Gal4 activation domain. Also tested in place of the latter were the Gal4 activation domain plasmid with no scDcp2n insert (control), a scDcp2ΔN fusion protein and mutant scDcp2n fusion proteins with single-amino acid substitutions in the N-terminal conserved patch. +His, growth on minimal selective plates containing histidine; +3AT, growth on minimal selective plates containing no histidine and 100 mM 3AT.

**Table 1**

## Data collection and refinement statistics

	Native <sup>a</sup>	SeMet <sup>a</sup>
<b>Data collection</b>		
Space group	<i>P</i> 16 <sub>1</sub>	<i>P</i> 6 <sub>1</sub>
Cell dimensions		
<i>a</i> , <i>b</i> , <i>c</i> (Å)	56.3, 56.3, 301.1	56.7, 56.7, 301.1
$\alpha$ $\beta$ $\gamma$ (°)	90, 90, 120	90, 90, 120
Resolution (Å)	2.5 (2.55–2.5) <sup>b</sup>	2.7 (2.75–2.7) <sup>b</sup>
<i>R</i> <sub>sym</sub> or <i>R</i> <sub>merge</sub> (%)	9.1(52.3)	9.6(46.4)
<i>I</i> / $\sigma$ <i>I</i>	21.9(4.0)	21.0(3.6)
Completeness (%)	100.0(100.0)	100.0(100.0)
Redundancy	10.0(7.5)	11.4(9.3)
<b>Refinement</b>		
Resolution range (Å)	20.0–2.5	
No. reflections	18,700	
<i>R</i> <sub>work</sub> / <i>R</i> <sub>free</sub>	25.0/28.7	
No. atoms		
Protein	3332	
Water	111	
<i>B</i> -factors (Å <sup>2</sup> )		
Protein	29.4	
Water	60.4	
R.m.s. deviations		
Bond lengths (Å)	0.012	
Bond angles (°)	1.32	

<sup>a</sup> One crystal is used for each data set.

<sup>b</sup> Values in the highest-resolution shell are shown in parenthesis.